Journal of Statistical Mechanics: Theory and Experiment
An IOP and SISSA journal

Granular micro-structure and avalanche precursors

Lydie Staron[1], **Farhang Radjai**[2] **and Jean-Pierre Vilotte**[3]

[1] Department of Applied Mathematics and Theoretical Physics, University of Cambridge, Cambridge CB3 0WA, UK
[2] Laboratoire de Mécanique et Génie Civil, Université Montpellier II, 34095 Montpellier, France
[3] Institut de Physique du Globe de Paris, 75252 Paris Cedex 5, France
E-mail: L.Staron@damtp.cam.ac.uk, radjai@lmgc.univ-montp2.fr and vilotte@ipgp.jussieu.fr

Received 22 May 2006
Accepted 13 June 2006
Published 31 July 2006

Online at stacks.iop.org/JSTAT/2006/P07014
doi:10.1088/1742-5468/2006/07/P07014

Abstract. We perform 2D numerical simulations to investigate the evolution of the internal state of a granular slope driven towards the stability limit. We first identify precursors of the avalanche and relate them to the intermittent mobilization of friction forces between the grains. Analysing the details of the micro-structure, namely the distribution of friction forces and the stress state at different scales, we give evidence of the existence of a preavalanche interval in which the micro-structure undergoes a sharp modification. Higher probability of precursors and the modification of the micro-structure occur in coincidence. The latter is discussed in terms of slope metastability and of the possible emergence of long-range correlations at the approach of the stability limit.

Keywords: granular matter, disordered systems (experiment), random/ordered microstructures (experiment), friction

J. Stat. Mech. (2006) P07014

1742-5468/06/P07014+15$30.00

Contents

1. Introduction

The trigger of a granular surface avalanche can be simply understood as the sudden loss of equilibrium of an upper layer of grains following a failure at any depth. Accordingly, balancing the weight of this upper layer along the slope with an effective friction force is sufficient to produce a stability condition, known as the Coulomb criterion [1]. This criterion establishes the existence of a plastic limit setting an upper bound for the granular slope: the static angle of repose, denoted θ_c in the following. Whenever the slope θ of a granular bed reaches θ_c, failure occurs and gives rise to a surface flow. The slope θ decreases accordingly and eventually reaches a lower value θ_d, known as the dynamical angle of repose, for which the flow stops and the granular bed stabilizes.

Both θ_c and θ_d can be related to mean effective frictional properties of the granular media. An effective coefficient of static friction can be simply defined through the relation $\mu_e = \tan\theta_c$. Its value primarily depends on the shape of the grains and the properties of the material they are made of [13]. It thus reflects local phenomena involving the scale of the grains. Accordingly, one expects the value of θ_c to be strongly dependent on the organization of the granular packing, i.e. its micro-structure (contact network geometry, force distribution), hence to be sensitive to the intrinsic disorder characterizing granular media in general. This sensitivity is apparent when measuring the value of θ_c for one given

doi:10.1088/1742-5468/2006/07/P07014

J. Stat. Mech. (2006) P07014

granular medium over successive avalanches: θ_c is not mono-valued, but distributed in a slope interval of few degrees [2]. In this slope interval, the macroscopic Coulomb criterion coincides with a maximum probability of avalanching, in which slight differences in the micro-structure might play a role.

The probability of triggering a surface avalanche when perturbing a granular slope was investigated experimentally. Daerr and Douady [4] measured the size of the perturbation necessary to trigger a surface flow depending on the slope θ of the surface. They found that the size of the perturbation tends towards zero when the slope tends towards θ_c, and that no surface flow can be triggered for $\theta < \theta_d$, thus characterizing the slope metastability as a sub-critical transition. On the other hand, it was shown that a perturbation of a given size applied to a granular slope induces a response of increasing amplitude when the slope θ evolves towards θ_c, while the response is rapidly damped when $\theta < \theta_d$ [5]. These experiments show the growing susceptibility of the pile to avalanching when approaching the static angle of friction θ_c, which it is tempting to attribute to the evolution of the micro-structure. However, beyond the observation of a metastable state in $[\theta_d, \theta_c]$, and the experimental evidence of precursors to the avalanche [12], the precise analysis of the state of the granular pile in this interval escapes the experimental tools.

In this contribution, we apply numerical simulation to investigate the evolution of the internal state of a granular slope driven towards the stability limit. We first identify precursors of the avalanche and relate them to the intermittent mobilization of friction forces between the grains. Analysing the details of the micro-structure, namely the distribution of friction forces and the stress state at different scales, we give evidence of the existence of a preavalanche interval in which the micro-structure undergoes a sharp modification. Occurrence of precursors and the modification of the micro-structure coincide in time. The latter is discussed in terms of the possible emergence of long-range correlations at the approach of the stability limit and slope metastability.

2. The numerical experiment

2.1. The contact dynamics

The numerical simulations were performed using a contact dynamics algorithm in 2D [8, 10]. This method assumes perfectly rigid grains interacting at contacts through a hard core repulsion and a Coulomb friction law. The friction law imposes that the tangential force f_t at any contact is bounded by the Coulomb threshold given by the normal force at contact f_n times the coefficient of inter-grain friction μ: $|f_t| \leq \mu f_n$ is satisfied at every contact point. In addition, the introduction of a coefficient of restitution e is required to control energy exchanges during binary collisions. Beyond the fact that contact dynamics treats them as strictly non-smooth, these contact laws do not essentially differ from those commonly used in other discrete simulations, molecular dynamics methods for instance [3]. Yet there exists an indetermination inherent to the contact dynamics: for one given configuration of grains and normal forces, different configurations of friction forces can be computed by the algorithm, inducing a randomness in the initial state. However, the initial configuration is rapidly erased by the loading of the system. Moreover, we are interested in the organization of forces as a result of loading and time evolution, through which indetermination vanishes. We thus expect the results reported hereafter to be robust against the simulation method.

J. Stat. Mech. (2006) P07014

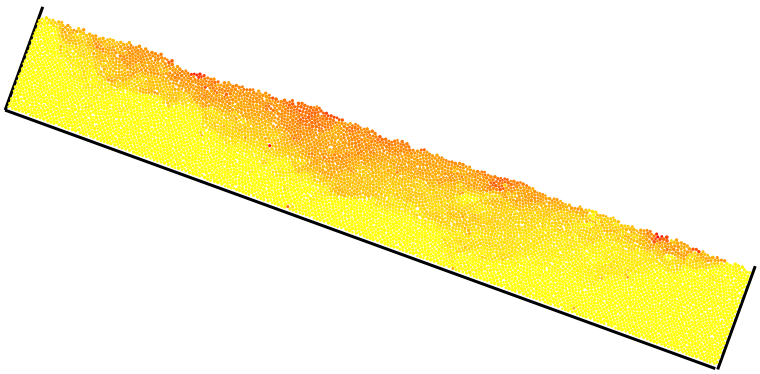

Figure 1. Granular bed with a width $L = 300D$ tilted at $\theta \simeq 20°$. Grains in red have a non-negligible velocity and show the start of an avalanche.

2.2. The simulation set-up

We consider circular disks of mean diameter D and showing a uniform size dispersity in a range such that $(D_{\max} - D_{\min})/D = 0.4$. By mean of random deposition in the gravity field, we build granular beds of depth $H = 40D$ and of width $L = 100D$, $150D$, $200D$, $250D$ and $300D$. However, the role of L in the behaviour of the systems is not systematically investigated. As we shall see, its influence on the results reported hereafter is weak. The number of grains used ranges from 4000 to 12 000. In all the simulations, the value of the inter-grain friction was set to $\mu = 0.5$ and was not varied; the value of the restitution coefficient is also constant, $e = 0$.

The numerical experiment consists of slowly tilting the granular beds in the gravity field at a constant rotation rate of $1° \text{ s}^{-1}$ so as to bring the slope θ of the free surface of the bed to the static angle of friction θ_c for which a surface avalanche occurs (see figure 1). We found $\theta_c \in [18°, 22°]$ over all the systems, but the influence of L on θ_c was not investigated. The pile stabilizes again for $\theta_d \in [14°, 17°]$. The quasi-static evolution towards the stability limit is analysed in terms of the existence of precursors and the evolution of the micro-structure.

3. Precursors of the incoming avalanche

3.1. The kinetic energy

The evolution of the mean kinetic energy of the grains is the first evidence of the existence of precursors to the granular avalanche. In figure 2 is reported the normalized translational kinetic energy of the grains $E_k/(\rho g D^3)$, where ρ is the surface density of the grains, for the two bed widths $L = 150D$ and $L = 250D$. We observe a noisy evolution showing bursts of activity soon after the tilting has started, and increasing in size while the slope tends towards θ_c. They show the existence of dynamical rearrangements within the bulk of grains occurring more and more frequently while the avalanche becomes incipient, for $\theta/\theta_c \gtrsim 0.7$, i.e. $\theta \gtrsim 15°$. Interestingly, this value compares with the value of θ_d. These dynamical rearrangements were experimentally observed by [12].

doi:10.1088/1742-5468/2006/07/P07014

J. Stat. Mech. (2006) P07014

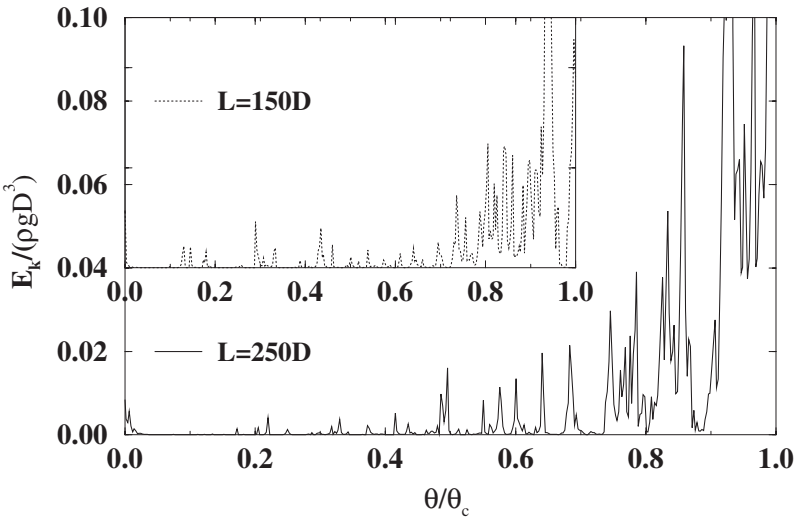

Figure 2. Normalized mean kinetic energy of the grains $E_k/\rho g D^3$ as a function of the normalized slope angle θ/θ_c for granular beds with $L = 250D$ (main graph) and $L = 150D$ (inset graph).

3.2. Reorganization of the contact network

In the first place, rearrangements of the grain packing, hence the evolution of the granular texture, simply result from the pile tilting. While the stress tensor shows an increasing deviator reflecting the shear loading undergone by the slope, we observe the slow emergence of a well defined anisotropy in the direction of the force chains, which tends to align following the main compressive direction [7, 9]. The geometrical network of contacts changes accordingly to adapt to the new stress state. This leads to the loss of contacts in some directions and the gain of contacts in others. The number of contacts gained and lost is roughly the same. Figure 3 shows for the different widths L the proportion of grains either lost or gained, $\Delta N/N$, where N is the total number of contacts, as a function of the slope angle normalized by the static angle of repose θ/θ_c. Beyond the time variations of $\Delta N/N$ for the different values of L, we observe an increasing activity in the slope interval of 3°–4° just preceding the stability limit, which can be materialized by a power-law envelope. This increasing activity however never involves more than 3% of the total number of contacts.

The distribution of contact orientations (in the pile referential) in the initial state is shown in figure 4. In spite of the grain size distribution, a clear signature of a hexagonal ordering can be seen through the existence of preferential directions at 0°, 60° and 120°. In the same figure are reported the distributions of the orientations where contacts are gained and contacts are lost in the slope interval of 3°–4° preceding the avalanche. We observe an asymmetry reflecting a shift of contacts from 60° to 120°, following the gravity direction.

3.3. Slip motion at contacts

A second form of dynamical rearrangements simply results from the possibility of slip motion between the grains in contacts, without necessarily leading to either loss or gain.

J. Stat. Mech. (2006) P07014

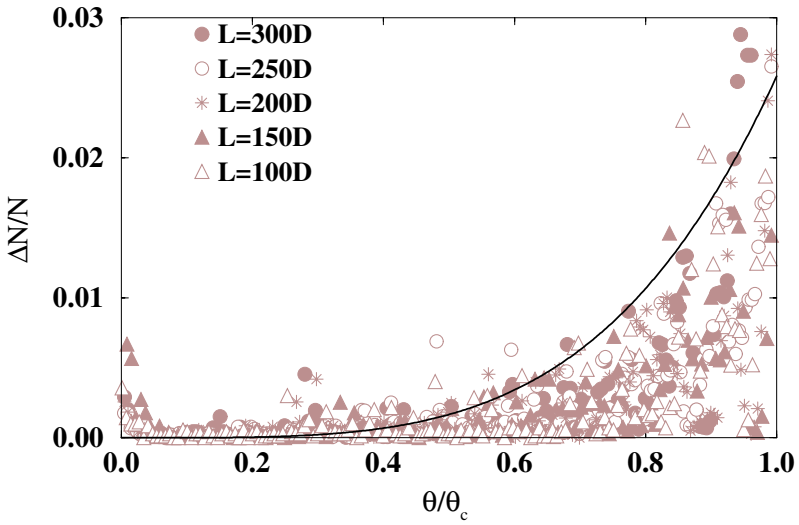

Figure 3. Proportion of contacts either lost or gained, $\Delta N/N$, as a function of the normalized slope angle θ/θ_c for granular beds with $L = 100D$, $150D$, $200D$, $250D$ and $300D$. The solid line shows a power-law envelope stressing the general increase of contact activity.

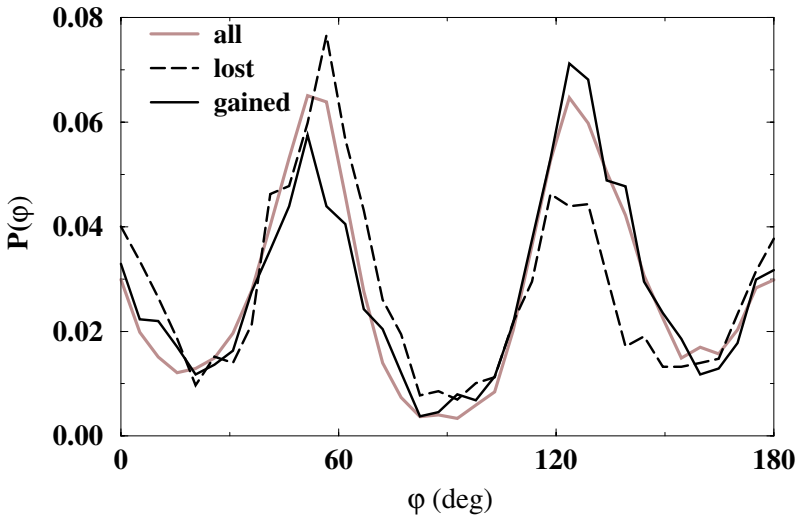

Figure 4. Normalized distributions of the orientations of the contacts either gained (solid line) or lost (dashed line) computed over the last four degrees of the pile evolution before the stability limit $\theta = \theta_c$ and for $L = 200D$. The grey solid line shows the normalized distribution of the orientations of *all* contacts in the initial state.

Indeed, the contacts between grains are ruled by a simple Coulomb friction law, which imposes an upper bound to the ratio of the tangential force to the normal force at contact: $|f_t/f_n| \leq \mu$, where μ is the coefficient of inter-grain friction. When the upper bound is reached, namely $|f_t/f_n| = \mu$, a relative slip motion at the contact is possible.

J. Stat. Mech. (2006) P07014

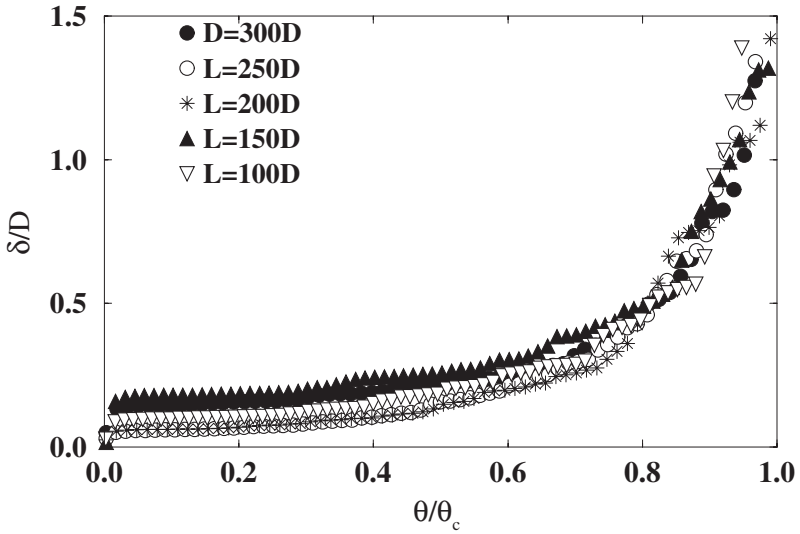

Figure 5. Normalized mean accumulated slip at contacts, δ/D, as a function of the normalized slope angle θ/θ_c for granular beds with $L = 100D$, $150D$, $200D$, $250D$ and $300D$.

While the pile is slowly tilted and the macroscopic shear stress gradually increases, more and more contacts will reach the Coulomb threshold and lead to a slip motion, provided the local state of the packing is compatible with this slip. If we compute the mean accumulated slip δ at contacts over the total time of the pile tilting and computed over all the contacts, we observe that the slip dynamics becomes much more important in an slope interval of few degrees before the pile reaches its stability limit (figure 5). Moreover, if we compute the accumulated slip δ_i occurring at each grain i, again computed over the whole duration of the tilting and considering all the contacts in which the grain i is involved, we observe that slip motion involves a large majority of grains. Figure 6 for instance shows the distribution of the δ_i for two systems with $L = 100D$ and $L = 300D$. Slip motion, and more generally mobilization of friction forces, appears thus to be the main source of rearrangements and avalanche precursors [11].

4. The mobilization of friction

4.1. Organization

While inducing slip motion at contacts, the mobilization of friction gives the packing large possibilities to rearrange itself and find locally new stable configurations. Meanwhile, it triggers local dynamical instabilities, which can degenerate into avalanches if the packing is unable to damp them, as can be the case in a metastable state. The organization of the friction forces is thus a major aspect of the evolution towards the stability limit. Understanding how it changes the structure of the packing and its response to any perturbation is a key aspect of avalanche triggering mechanisms.

The interplay between the organization of friction forces and the granular texture is illustrated in figure 7, where a polar diagram of the contacts orientation and a polar diagram of the friction mobilization $|f_t|/f_n$ can be compared. While the anisotropy of

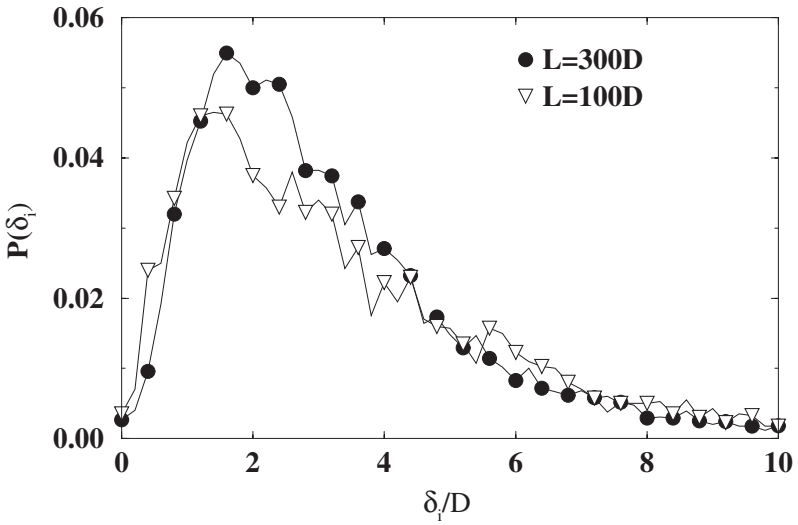

Figure 6. Distribution of normalized accumulated slip δ_i involving grain i computed over the whole duration of the tilting and for granular beds with $L = 100D$ and $L = 300D$.

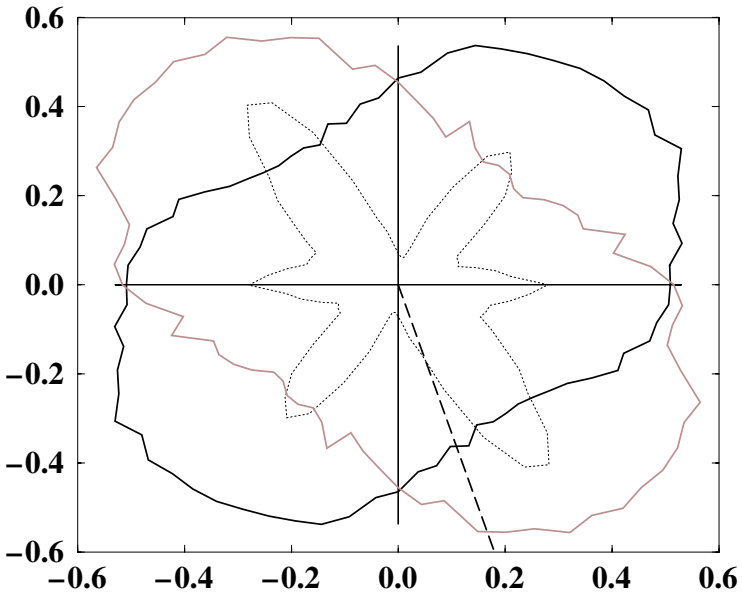

Figure 7. Polar distribution of the contact orientations (dotted line), of the normalized normal force f_n (solid grey line), and of the mean friction mobilization carried by the contacts $f_t/\mu f_n$ (solid black line) in the slope interval of 3° preceding the avalanche. The dashed line shows the direction of gravity, namely the main compressive direction (from [16]).

contact orientation essentially follows the main compressive direction, the anisotropy of friction mobilization is nearly orthogonal to it. These different anisotropies coincide with the fact that friction is mostly mobilized at weak contacts, namely contacts transmitting forces of intensity lower than the mean, while force chains carrying intense forces are

doi:10.1088/1742-5468/2006/07/P07014

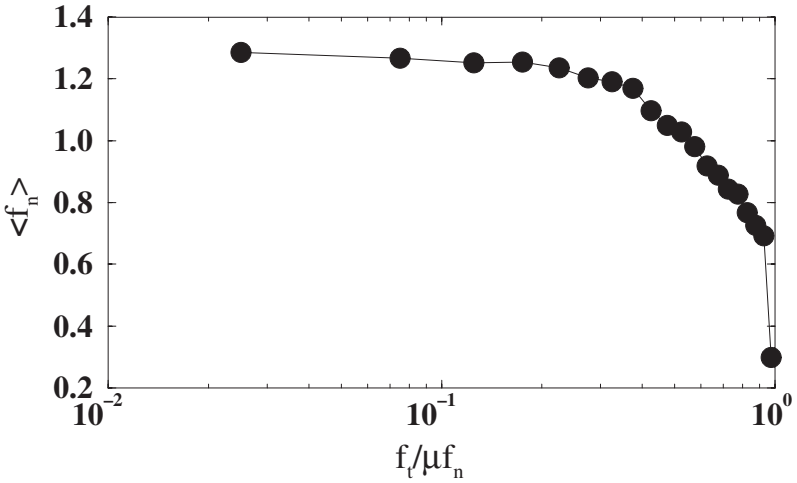

Figure 8. Mean intensity of the normal force $\langle f_\mathrm{n}\rangle$ carried by contacts of friction mobilization $f_\mathrm{t}/\mu f_\mathrm{n}$: we observe that larger friction mobilization coincides on average with weaker forces.

only marginally affected by friction mobilization [16]. This particular feature is visible in figure 8, where the mean normal force associated with a friction mobilization of $|f_\mathrm{t}|/\mu f_\mathrm{n}$ is plotted at an instant closely preceding the onset of an avalanche. We observe that, in the mean, high friction coincides with weaker forces. As a result, the evolution of contact friction is not reflected by the mean stress tensor, but requires to be analysed at local to mesoscopic scales.

4.2. The critical contacts

The ability of friction forces to trigger local instabilities depends on how much friction is mobilized at each contact. Where $|f_\mathrm{t}| < \mu f_\mathrm{n}$, no slip motion can occur and the contact is stable in the sense that it will not give rise to any local instability. However, while the pile is slowly tilted, the tangential force $|f_\mathrm{t}|$, at some contacts, incrementally increases and eventually reaches the Coulomb threshold $|f_\mathrm{t}| = \mu f_\mathrm{n}$. A slip motion is very likely to occur accordingly, possibly causing neighbouring contacts to reach the Coulomb threshold and slip in their turn. A possible quantity to measure the probability of such events is the proportion or density ν of contacts such that $|f_\mathrm{t}| = \mu f_\mathrm{n}$, referred to as critical in the following. The density ν is simply given by

$$\nu = \frac{N_\mathrm{c}}{N}, \tag{1}$$

where N_c is the number of critical contacts and N is the total number of contacts. Practically, critical contacts are identified as such when $|f_\mathrm{t}| = \mu f_\mathrm{n}(1-\epsilon)$ with $\epsilon = 0.01$. However, critical contacts form a well defined population and actually coincide with a singularity [16]. As a result, ν is only weakly affected by the value of ϵ. An example of the evolution of ν computed over the whole volume of the granular bed is shown in figure 9 for $L = 100D$ and $L = 300D$. The intermittent behaviour reveals a stick–slip dynamics where important variations of ν suggest a collective, or strongly correlated,

J. Stat. Mech. (2006) P07014

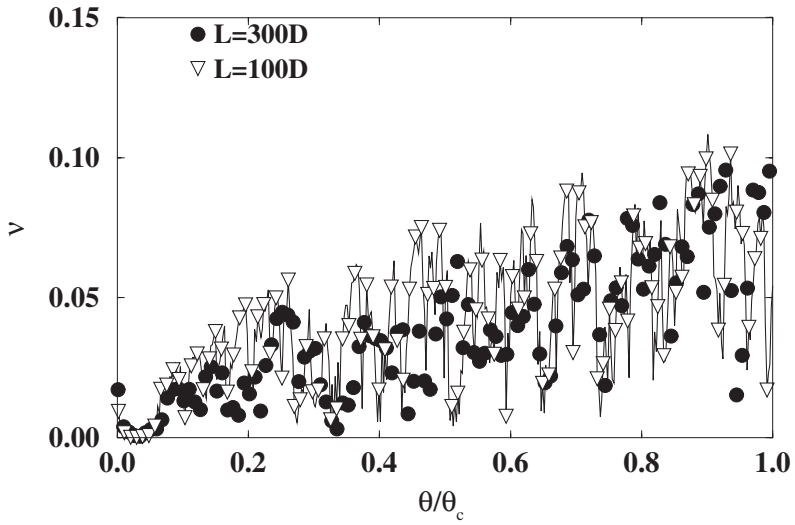

Figure 9. Time evolution of the density of critical contacts ν as a function of the normalized slope angle θ/θ_c for granular beds of width $L = 100D$ and $300D$.

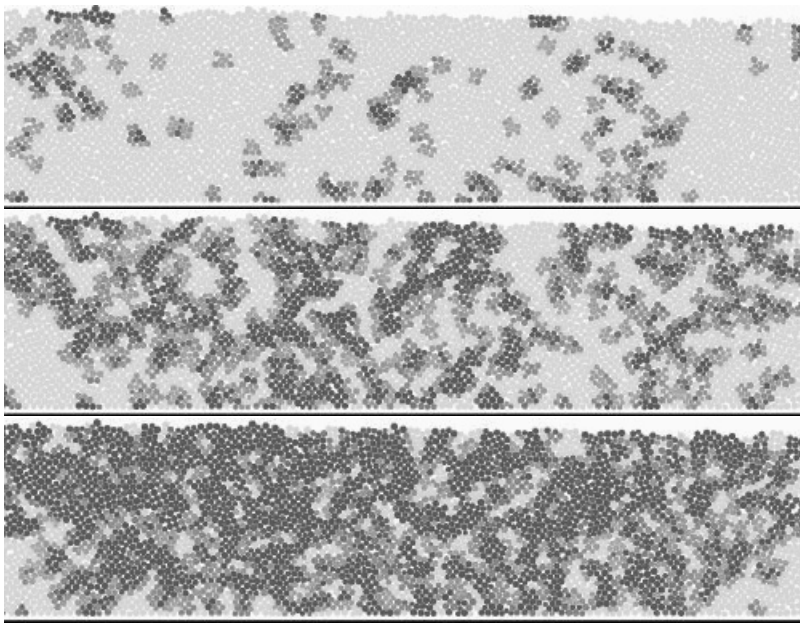

Figure 10. Snapshots of the pile for $\theta = 10°$, $16°$ and θ_c. In black are represented the areas where the critical contact density satisfies $\nu \geq \nu_c$.

behaviour. Analysing correlations between the values reached by ν and the existence of rearrangements in the packing, one can identify a limit density ν_c compatible with equilibrium. For $\nu > \nu_c$ larger scale rearrangements threaten the overall stability of the packing [14]. Figure 10 shows snapshots of a pile where the local values of ν is computed by averaging in a neighbourhood of radius $5D$ around each particle, and is indicated following a grey-level scale. One can see the appearance of a pattern and the growing size of the clusters of critical contacts, inducing locally $\nu = \nu_c$. This evolution, reminiscent

doi:10.1088/1742-5468/2006/07/P07014

J. Stat. Mech. (2006) P07014

of a percolation mechanism, also suggests the emergence of long-range correlations in proximity to the stability limit.

4.3. A dynamical response

The critical contacts form a well defined subset revealing the complexity of the structure of the packing when approaching failure. The existence of these contacts is closely linked with the loading applied, so that their behaviour will partly reflect the latter. For instance, the frequency of the stick–slip dynamics will increase for lower tilting velocity. In contrast, when stopping the tilting, one can observe that critical contacts rapidly relax and their density drops to zero [6]. Their density should thus be seen as a dynamical response of the pile to an external loading rather than as an actual variable describing the internal state of the packing. This dynamical response is very likely to reflect the state of friction mobilization and the existence of correlations between contacts. However, an extensive study of friction forces and their evolution is necessary to achieve a comprehensive picture of the state of the pile, and to understand its response to loading and to perturbations.

5. Multi-scale analysis of the stress

The existence of an interval of slope angle in which precursors occur more and more frequently is essentially related to the mobilization of friction forces, as stressed in the previous section. But mobilization of friction does not coincide with the transmission of intense forces. As a result, the signature of the friction induced precursors in the evolution of the macroscopic stress is very slight, and further analysis of the stress state at smaller scales is necessary to characterize the evolution of the micro-structure.

5.1. Definition

To evaluate the stress state of the packing, we use the concept of grain moment tensor defined in [10]. We consider a grain p involved in N_α contacts with neighbouring grains, and subjected to the forces $\mathbf{f}^\alpha$ applied at the contact points $\mathbf{r}^\alpha$. The moment tensor $\mathbf{M}_p$ of the grain p is given by

$$M_{ij}(p) = \sum_{\alpha=1,N_\alpha} r_i^\alpha f_j^\alpha, \tag{2}$$

where i and j are the space dimensions. Using the additivity of the moment tensor, we compute the tensor $\mathbf{M}$ of the pile taking into account all the grains. The moment tensor is related to the stress tensor through the relation $\sigma = \mathbf{M}/V$, where V is the volume over which the tensor is evaluated. In the following we consider ratios of stress component so that the definition of the volume is not required. Using the eigenvalues of the moment tensor m_1 and m_2, we compute the deviatoric part $Q = (m_1 - m_2)/2$ and the isotropic part $P = (m_1 + m_2)/2$. We form the ratio of these two quantities

$$\Gamma = \frac{Q}{P}, \tag{3}$$

i.e. the level of deviatoric stress normalized by the pressure.

J. Stat. Mech. (2006) P07014

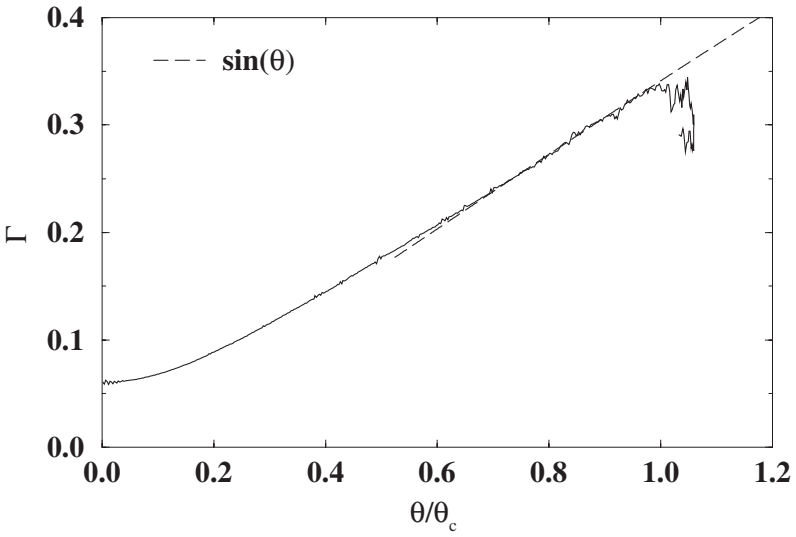

Figure 11. Evolution of the macroscopic stress ratio Γ as a function of the normalized slope angle θ/θ_c; it follows the classical prediction at failure $\Gamma(\theta_c) = \sin(\theta_c)$ (dashed line).

5.2. The macroscopic stress

The evolution of the ratio Γ evaluated over the whole volume of the pile as a function of the slope angle θ is reported in figure 11 for the granular bed with $L = 300D$. While the slope evolves towards θ_c, the monotonic increase of Γ shows the gradual loading of the slope and the increase of shear stress following a classical evolution. No effect of the walls can be perceived on this evolution because the width L of the pile is large enough. We have checked however that the results reported hereafter on the multiscale analysis of the stress were independent of L [15]. For $\theta = \theta_c \simeq 20°$, the regular increase stops and softening of the material occurs. We define the corresponding limit stress state

$$\Gamma_c = \frac{Q}{P}(\theta_c). \tag{4}$$

Even though fluctuations can be observed before θ reaches the value of θ_c, the smooth evolution of Γ gives no indication of the way the pile reaches the plastic limit Γ_c.

5.3. Grain stresses

We define for each grain the stress ratio

$$\gamma = \frac{q}{p}, \tag{5}$$

where q and p are the deviatoric and isotropic part of the grain moment tensor given by equation (2). We focus on the *overloaded grains*, namely the grains satisfying $\gamma \geq \Gamma_c$. Three snapshots of the pile with $L = 300D$ for $\theta = 0$, 10° and θ_c are shown in figure 12; on these snapshots, the overloaded grains only are represented in black. In the course of time, we observe a slow structuring of the packing reminiscent of a percolation process, and which can be compared with the evolution of the friction mobilization displayed in

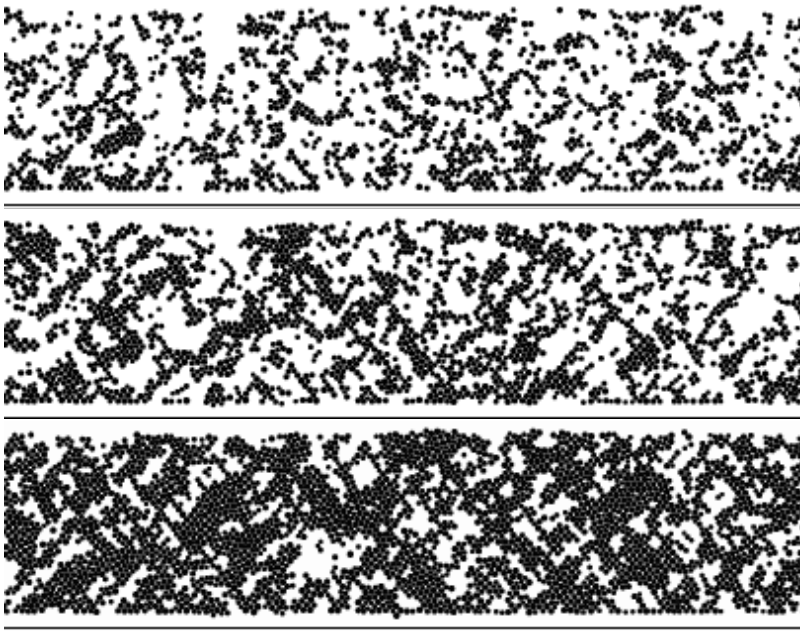

Figure 12. Snapshots of the pile for $\theta = 0°$, $10°$ and θ_c. In black are represented the overloaded grains satisfying $\gamma \geq \Gamma_c$, where $\gamma = q/p$ is computed from the grain moment tensor (from [15]).

figure 10. We can indeed suspect the organization of the local momentum to be related to the organization of friction forces, which locally induce strong deviatoric load.

5.4. Multi-scale analysis

To characterize the pattern shown in the snapshots of figure 12, we consider the emergence of areas where the stress state has reached the macroscopic plastic limit Γ_c, and follow their evolution. Therefore we compute the maximum size $\ell_c^{\max}$ of these areas in the course of time focusing on the overloaded grains. For each overloaded grain, we consider a circular neighbourhood of radius ℓ over which the stress state is evaluated. We can thus determine the size of the neighbourhood ℓ_c for which the stress state satisfies $\Gamma = \Gamma_c$. Carrying this operation over all the overloaded grains we are able to determine $\ell_c^{\max} = \max\{\ell_c\}$ for any value of the slope θ. The evolution of $\ell_c^{\max}$ as a function of θ is plotted in figure 13. We first observe a slow increase for $\theta \in [0°, 15°]$. At $\theta \simeq 15°$, a rapid jump suddenly brings $\ell_c^{\max}$ to $30D$, namely a size comparable to the packing height (this maximum value $30D$ is imposed as a cut-off for practical reasons in the computation of ℓ_c, which otherwise would reach the pile dimension $40D$). Again, this behaviour is reminiscent of a percolation mechanism in the sense that potentially unstable areas suddenly become connected. Following this picture, it clearly establishes the existence of a transition in the stress state of the packing few degrees (here $5°$) before the angle of avalanche θ_c is reached: 'plastic' zones (where $\Gamma = \Gamma_c$) emerge from local scale to macroscopic scale. In addition to the fact that this transition in itself is a strong precursor to the avalanche, we can suspect it to deeply affect the pile's susceptibility to avalanching.

J. Stat. Mech. (2006) P07014

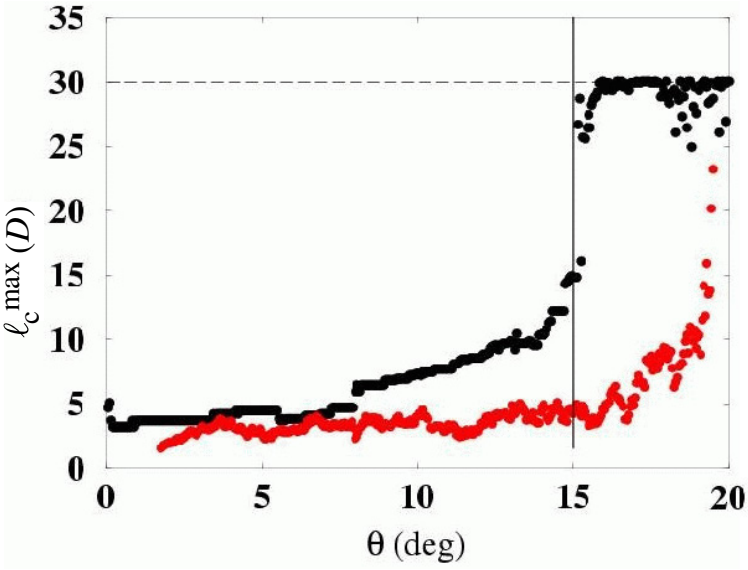

Figure 13. Evolution of the maximum radius ℓ_c^{max} of the areas where $\Gamma = \Gamma_c$ is satisfied (black circles) and evolution of the mean size of the clusters of critical contacts where $\nu = \nu_c$ is satisfied as a function of the slope angle θ; we observe a slope interval $\Delta\theta \simeq 5°$ in which the system undergoes a transition.

6. Discussion: micro-structure and metastability

The detailed analysis of numerical simulations of the quasi-static evolution of granular beds towards the stability limits allows for new important insights in the destabilization process. First, we give evidence of precursors of increasing size mainly related to the mobilization of friction forces, and occurring in a slope interval of a few degrees preceding the angle of avalanche θ_c. Then, an accurate study of the mobilization of friction forces and of the stress state at local and meso-scales shows the slow structuring of the packing. On one hand, growing clusters of critical contacts make any local perturbation likely to propagate through the slip motion of neighbouring contacts, thus increasing the probability of triggering an avalanche. On the other hand, areas where the stress state has reached the macroscopic plastic limit increase in size and eventually span the granular bed so as to possibly threaten its stability. These modifications of the granular micro-structure can be interpreted as the emergence of long range correlations in the packing, but this conclusion requires further analysis. In any case, the irreversibility of these modifications, and their influence on the hysteretic behaviour of the packing, were shown in [6].

Both clusters of critical contacts and mesoscale stress state point at a slope interval of few degrees before stability limit as a transition in their behaviour. This transition can be seen in figure 13 where the evolution of the maximum radius ℓ_c^{max} of the areas where $\Gamma = \Gamma_c$ is satisfied and the evolution of the mean size of the clusters of critical contacts where $\nu = \nu_c$ is satisfied are both represented. We thus observe a strong correlation between the probability of occurrence of precursors and the evolution of the micro-structure.

This preavalanche interval, of a few degrees in the case of our simulations, compares well with the hysteresis angle $\theta_c - \theta_d$, in which the slope metastability was experimentally

J. Stat. Mech. (2006) P07014

evidenced. Although the existence of new correlation lengths in this interval has still to be rigorously established, it is tempting to identify the origin of the metastability with the modification of the internal state of the pile.

References

[1] Coulomb C-A, 1773 *Acam. R. Sci. Mem. Math, Phys. par Divers Savants* **7** 343
[2] Courrech du Pont S, Gondret P, Perrin B and Rabaud M, *Granular avalanches in fluids*, 2003 *Phys. Rev. Lett.* **90** 044301
[3] Cundall P A and Stack O D L, 1979 *Geotechnique* **29** 47
[4] Daerr A and Douady S, *Two types of avalanche behaviour in granular media*, 1999 *Nature* **399** 241
[5] Deboeuf S, Bertin E M, Lajeunesse E and Dauchot O, *Jamming transition of a granular pile below the angle of repose*, 2003 *Eur. Phys. J.* B **36** 105
[6] Deboeuf S, Dauchot O, Staron L, Mangeney A and Vilotte J-P, *Memory of the unjamming transition during cyclic tiltings of a granular pile*, 2005 *Phys. Rev.* E **72** 051305
[7] Snoeijer J H, Ellenbroek W G, Vlugt T J H and van Hecke M, *Sheared force networks: anisotropies, yielding, and geometry*, 2006 *Phys. Rev. Lett.* **96** 098001
[8] Jean M and Moreau J-J, *Unilaterality and dry friction in the dynamics of rigid body collections*, 1992 *Proc. Contact Mech. Int. Symp.* pp 31–48
[9] Majmudar T S and Behringer R P, *Contact force measurements and stress-induced anisotropy in granular materials*, 2005 *Nature* **435** 1079
[10] Moreau J-J, *Numerical investigation of shear zones in granular materials*, 1997 *Friction, Arching, Contact Dynamics* (Singapore: World Scientific) pp 233–47
[11] Nasuno S, Kudrolli A and Gollub J P, 1997 *Phys. Rev. Lett.* **79** 949
[12] Nerone N, Aguirre M A, Calvo A, Bideau D and Ippolito I, *Instabilities in slowly driven granular packing*, 2003 *Phys. Rev.* E **67** 011302
[13] Pöschel T and Buchholtz V, *Static friction phenomena in granular materials: Coulomb law versus particle geometry*, 1993 *Phys. Rev. Lett.* **71** 3963
[14] Staron L, Vilotte J-P and Radjai F, *Pre-avalanche instabilities in a granular pile*, 2002 *Phys. Rev. Lett.* **89** 204302
[15] Staron L, Radjai F and Vilotte J-P, *Multiscale analysis ot the stress state in a granular slope in transition to failure*, 2005 *Eur. Phys. J.* E **18** 311
[16] Staron L and Radjai F, *Friction versus texture at the approach of a granular avalanche*, 2005 *Phys. Rev.* E **72** 041308

J. Stat. Mech. (2006) P07014